Cellular/Molecular

In Vivo Assessment of Brain Interstitial Fluid with Microdialysis Reveals Plaque-Associated Changes in Amyloid-β Metabolism and Half-Life

John R. Cirrito,[1] Patrick C. May,[4] Mark A. O'Dell,[1] Jennie W. Taylor,[1] Maia Parsadanian,[1] Jeffrey W. Cramer,[5] James E. Audia,[6] Jeffrey S. Nissen,[6] Kelly R. Bales,[4] Steven M. Paul,[4,7] Ronald B. DeMattos,[4] and David M. Holtzman[1,2,3]

Departments of [1]Neurology and [2]Molecular Biology and Pharmacology and [3]Center for the Study of Nervous System Injury, Washington University School of Medicine, St. Louis, Missouri 63110, [4]Neuroscience Discovery Research and [5]Drug Disposition-Lead Optimization, [6]Discovery Chemistry Research, Eli Lilly and Company, Lilly Research Laboratories, Indianapolis, Indiana 46285, and [7]Departments of Pharmacology, Toxicology, and Psychiatry, Indiana University School of Medicine, Indianapolis, Indiana 46285

Soluble amyloid-β (Aβ) peptide converts to structures with high β-sheet content in Alzheimer's disease (AD). Soluble Aβ is released by neurons into the brain interstitial fluid (ISF), in which it can convert into toxic aggregates. Because assessment of ISF Aβ levels may provide unique insights into Aβ metabolism and AD, an *in vivo* microdialysis technique was developed to measure it. Our Aβ microdialysis technique was validated *ex vivo* with human CSF and then *in vivo* in awake, freely moving mice. Using human amyloid precursor protein (APP) transgenic mice, we found that, before the onset of AD-like pathology, ISF Aβ in hippocampus and cortex correlated with levels of APP in those tissues. After the onset of Aβ deposition, significant changes in the ISF $Aβ_{40}/Aβ_{42}$ ratio developed without changes in $Aβ_{1-x}$. These changes differed from changes seen in tissue lysates from the same animals. By rapidly inhibiting Aβ production, we found that ISF Aβ half-life was short (~2 hr) in young mice but was twofold longer in mice with Aβ deposits. This increase in half-life, without an increase in steady-state levels, suggests that inhibition of Aβ synthesis reveals a portion of the insoluble Aβ pool that is in dynamic equilibrium with ISF Aβ. This now measurable *in vivo* pool is a likely target for new diagnostic and therapeutic strategies.

Key words: **Alzheimer; amyloid; interstitial fluid; microdialysis; half-life; gamma-secretase**

Introduction

Genetic, biochemical, and animal model studies strongly suggest a central role for amyloid-β (Aβ) in the pathogenesis of Alzheimer's disease (AD) (Sisodia, 1999; Golde et al., 2000; St. George-Hyslop, 2000; Selkoe, 2001). Aβ is a 38–43 amino acid peptide derived from the amyloid precursor protein (APP). Early-onset forms of familial, autosomal dominant AD appear to be attributable to an overproduction of a more amyloidogenic form of Aβ ($Aβ_{42}$), resulting in conversion of Aβ, in early adult life, from soluble, nontoxic forms to both soluble and insoluble toxic forms with a high β-sheet content (Tanzi et al., 1996). In contrast, the most common form of AD (late-onset, age >60) does not appear to result from Aβ overproduction. Instead, other genetic [e.g., *APOE* (apolipoprotein E) allelic differences] and nongenetic factors appear to be important in determining whether and when Aβ conformational changes occur (Wisniewski et al., 1997; Teplow, 1998; Holtzman, 2001). Thus, understanding not only mechanisms of Aβ production but also factors that control Aβ metabolism are likely to be critical for understanding AD pathogenesis, as well as for developing better diagnostic and treatment methods.

A major pathologic hallmark of AD is the deposition of the normally soluble Aβ peptide into aggregated, extracellular structures called plaques (Price et al., 1998; Selkoe, 2001). Although it is not proven whether the seed, or nidus, of plaques originates extracellularly or intracellularly, recent evidence suggests that initial formation and growth of plaques can occur extracellularly (Meyer-Luehmann et al., 2003). Regardless of where plaques originate, it is likely that the subsequent Aβ building blocks for plaques are derived from the brain interstitial fluid (ISF). Aβ appears to be released from neurons into the extracellular space normally via synaptic activity (Kamenetz et al., 2003). Assessment of the ISF pool of Aβ may provide unique insights into the regulation of Aβ metabolism, Aβ aggregation, and plaque formation. To date, however, there have been no methods that have permitted analysis of ISF Aβ.

To this end, we developed an *in vivo* microdialysis technique to measure ISF Aβ in awake, APP transgenic mice that develop age-dependent Aβ aggregation and deposition (PDAPP mice) (Games et al., 1995). We compared the steady-state concentrations of several Aβ species in the ISF of 3-month-old and 12- to 15-month-old PDAPP mice to those species within the CSF and

Received June 11, 2003; revised Aug. 4, 2003; accepted Aug. 4, 2003.

This work was supported by National Institutes of Health Grants AG13956, AG11355, and AG20222, MetLife Foundation, and Eli Lilly and Co. We thank the Washington University General Clinical Research Center (funded by United States Public Health System Grant M01 RR00036).

Correspondence should be addressed to Dr. David M. Holtzman, Washington University School of Medicine, Department of Neurology, 660 South Euclid Avenue, Box 8111, St. Louis, MO 63110. E-mail: holtzman@neuro.wustl.edu.

 0270-6474/03/238844-10$15.00/0

tissue. These studies show that the development of Aβ deposition is associated with changes in ISF Aβ levels and ratios that differ in relation to tissue lysates and CSF. By combining our microdialysis technique with a potent γ-secretase inhibitor, we also demonstrate that the half-life of ISF Aβ is short and is markedly influenced by the presence of Aβ deposition. This strongly suggests that rapid inhibition of Aβ production *in vivo* reveals an equilibrium between soluble and part of the insoluble pool of Aβ. This rapidly dissociable, now measurable pool of Aβ may provide new ways to diagnose the presence of Aβ deposits and is likely to be the target of various anti-Aβ treatments.

Materials and Methods

In vitro *microdialysis.* Microdialysis probes used for *in vitro* experiments had a 4 mm, 35 kDa molecular weight cutoff (MWCO) membrane (BR-4–10 probes; Bioanalytical Systems, West Lafayette, IN) and were connected to a microdialysis peristaltic pump (MAB20; SciPro, Sanborn, NY) using teflon (FEP) tubing (inner diameter, 0.12 mm; 1.2 μl/10 cm; SciPro). Before use, probes were washed with 0.15% bovine serum albumin (BSA)–artificial CSF (aCSF) perfusion buffer (in mM: 1.3 $CaCl_2$, 1.2 $MgSO_4$, 3 KCl, 0.4 KH_2PO_4, 25 $NaHCO_3$, and 122 NaCl, pH 7.35) that was filtered through a 100 kDa MWCO membrane (Millipore, Billerica, MA). *In vitro* studies using samples of human CSF were collected by lumbar puncture from cognitively normal research volunteers from the Washington University Memory and Aging Project as described previously (Fagan et al., 2000). The study was approved by the Human Studies Committee at Washington University. Samples were stored at 4°C in polypropylene tubes.

Interpolated zero flow method. A 0.15% BSA–aCSF perfusion buffer was passed through a microdialysis probe immersed in human CSF. Flow rates ranged from 0.5 to 2.6 μl/min. The concentration of $A\beta_{1\text{-}x}$ obtained in each microdialysis sample was measured by ELISA. The actual concentration of exchangeable Aβ (eAβ) in each sample was assessed by plotting the sample Aβ concentration versus the flow rate and then extrapolating back to a zero flow rate to determine the concentration of eAβ within the target CSF. For each flow rate, the percentage recovery was determined by the following: $(C_x/E) * 100$, where C_x is the concentration of Aβ in the dialysate at a given flow rate, and E is the calculated concentration of eAβ in that sample.

Animals. All experimental procedures involving animals were performed in accordance with guidelines established by the Animal Studies Committee at Washington University. PDAPP mice homozygous for the APP^{V717F} transgene (Games et al., 1995; Bales et al., 1997) were bred to Swiss Webster mice (Charles River Laboratories, Wilmington, MA) to produce PDAPP hemizygous transgenic mice. Animals were used at 3–4 months of age (young) or 12–15 months of age (middle-aged). C57BL/6 mice were purchased from Harlan Sprague Dawley (Indianapolis, IN).

In vivo *microdialysis technique.* Microdialysis probes used for *in vivo* experiments had a 4 mm, 38 kDa MWCO membrane (MBR-4–10 probes; Bioanalytical Systems) and were connected to a Univentor 864 syringe pump (SciPro). Before guide implantation surgery, probes were prepared as stated above. For microdialysis guide cannula implantation, PDAPP mice were anesthetized using 1.5–2.5% isoflurane. The head was shaved, and the skin was transected along the midline to expose the skull from several millimeters anterior and posterior to bregma and lambda. The animal was then placed in a small animal stereotaxic device equipped with dual manipulator arms and an anesthetic mask (David Kopf Instruments, Tujunga, CA). To ensure the skull was level for each animal, measurements and adjustments were made so that bregma and lambda were at equal heights (with 0.1 mm tolerance), as well as 2 points equidistant from midline. Bore holes (0.75 mm) were made above the left hippocampus (coordinates, bregma −3.1 mm, 2.4 mm lateral, −0.6 mm relative to dura mater) and above the right striatum (coordinates, bregma +0.2 mm, 2.2 mm lateral, −0.5 mm relative to dura mater). An additional bore hole was made into the right, posterior skull quadrant for an anchoring bone screw. MBR-10 guide cannulas (Bioanalytical Systems) were stereotactically inserted into the hippocampus (12° angle) and striatum (0° angle) and cemented into place using a binary dental cement. Once the cement was firm, the animal was removed from the stereotaxic device, and the wound was closed anterior and posterior to the guide assembly using 1.75 mm Michel suture clips (Fine Science Tools, Foster City, CA).

The guide cannula stylets were removed, and the flushed microdialysis probes were manually inserted through the guide cannula into the target regions. After probe insertion, mice were fitted with a plastic mouse collar and placed into cages designed to allow unrestricted movement of the animal without applying pressure to probe assembly (Raturn Cage System; Bioanalytical Systems). Animals were then allowed to awaken and remained awake for remainder of the experiment. To measure $A\beta_{1\text{-}x}$, microdialysis probes had a constant flow rate of 2.6 μl/min. Microdialysis samples were collected hourly or bihourly using a refrigerated fraction collector.

At the conclusion of the microdialysis experiment, animals were anesthetized with 60 mg/kg Nembutal. CSF was collected from the cisterna magna (DeMattos et al., 2002b). Plasma was sampled via cardiac bleed, and the animal was perfused with cold PBS–heparin. The brain was fixed overnight in 4% paraformaldehyde at 4°C and then transferred to 30% sucrose. Brains sections (40 μm) were cut on a freezing microtome. All probe placements were verified by cresyl violet staining. Microdialysis samples were kept at 4°C and analyzed the day of collection by ELISA. Data from probe placements outside the appropriate region were discarded.

To assess ISF eAβ via microdialysis, as well as tissue Aβ levels in the same animal, a subset of mice received only unilateral hippocampal probes. To measure $eA\beta_{40}$ and $eA\beta_{42}$, a single fraction was collected from hours 4 to 10 after probe implantation at a flow rate of 0.5 μl/min. This protocol enriched the fraction for Aβ and facilitated individual Aβ species to be detected by ELISA. At the conclusion of the experiment, the implanted hemisphere was fixed and processed for histology to verify probe placement and quantify percentage Aβ load by immunostaining, whereas the contralateral hemisphere was dissected for several brain regions and processed for biochemical analysis.

Aβ quantification. Microdialysis samples, CSF, and tissues were analyzed for Aβ using a denaturing, sandwich ELISA specific for human $A\beta_{1\text{-}x}$, $A\beta_{1\text{–}40}$, or $A\beta_{1\text{–}42}$ (see Fig. 2*A*). The $A\beta_{1\text{-}x}$ ELISA measures $A\beta_{1\text{-}x}$ by using a central-domain monoclonal antibody (m266) against amino acids 13–28 as a capture antibody. To capture the different species of full-length Aβ, C-terminal domain monoclonal antibodies specific for either $A\beta_{40}$ (m2G3) or $A\beta_{42}$ (m21F12) were used. All assays used a biotinylated N-terminal domain monoclonal antibody specific for an intact N terminus (amino acids 1–5) of human Aβ (m3D6) as a reporting antibody, followed by streptavidin–poly-horseradish peroxidase-20 (Research Diagnostics, Flanders, NJ). C-Terminal variants of human Aβ (Aβ-CTV) are a calculation of the $A\beta_{40}$ and $A\beta_{42}$ ELISA values subtracted from the mean concentration from the $A\beta_{1\text{-}x}$ ELISA. This would include any peptide species that start at amino acids 1 through 28 or longer but does not end in amino acid 40 or 42. Murine $A\beta_{40}$ and murine $A\beta_{42}$ were detected using either m266 or m21F12 as a capture antibody and biotinylated m2G3 or m266 to detect. Slow ELISA TMB (Sigma, St. Louis, MO) was used for colorimetric detection and analyzed on a BioTek (Winooski, VT) 600FL microtiter plate reader. $A\beta_{40}$ and $A\beta_{42}$ standard curves were generated from Aβ peptide obtained from American Peptide (Sunnyvale, CA).

All ELISA samples were diluted in a final buffer of 0.25% BSA–500 mM guanidine–200 mM Tris–PBS, pH 7.4 with protease inhibitors. Microdialysis sample concentrations were corrected for *in vivo* percentage recovery based on the flow rate at which the sample was collected (example, 2.6 μl/min = 4.9% recovery and 0.5 μl/min = 56.3% recovery). Hippocampal tissues were processed by a sequential Aβ extraction using a 0.1 M carbonate buffer, pH 11.5, followed by a 5 M guanidine extraction of the pellet as described previously (DeMattos et al., 2002c). Tissue sample concentrations were normalized to protein concentration as measured by Micro BCA Assay (Pierce, Rockford, IL).

Acid–urea PAGE and Western blot. A single, 24 hr hippocampal microdialysis sample was collected at 0.5 μl/min from a 3-month-old PDAPP mouse. This sample was then immunoprecipitated with biotinylated m266, followed by streptavidin Sepharose beads (Amersham Bio-

sciences, Piscataway, NJ). Aβ was eluted from the pellet with 100% formic acid, diluted in loading dye, and loaded onto a 22% acid–urea polyacrylamide gel (DeMattos et al., 2001, 2002c). The gel was run at 275 V overnight in a glacial acetic acid running buffer and then transferred to nitrocellulose. The membrane was incubated overnight at room temperature with m3D6 and then probed with sheep anti-mouse horseradish peroxidase (Amersham Biosciences) for 3 hr, followed by SuperSignal West Pico Chemiluminescence (Pierce). Image was captured using the Kodak ImageStation 440CF (Eastman Kodak, Rochester, NY). Densitometry and standard curves were generated using the Kodak 1D Image Analysis software.

Determination of Aβ load. Tissue sections (40 μm) were cut using a freezing sliding microtome. Aβ was identified using a rabbit polyclonal antibody against pan-Aβ (BioSource International, Camarillo, CA). Percentage Aβ load was determined using stereological techniques in the cingulate cortex and hippocampus of three sections separated by 300 μm (Holtzman et al., 2000; DeMattos et al., 2002c). Quantification was performed anterior to probe placement.

ISF Aβ half-life determination–γ-secretase inhibitor treatment. ISF $Aβ_{1-x}$ half-life was determined in animals implanted with microdialysis probes as above. One hour baseline samples were taken from hours 5–8 after probe implantation. At the beginning of hour 9, animals were briefly anesthetized with isoflurane and injected subcutaneously with vehicle or 3 mg/kg LY411575 (Wu et al., 1998) diluted in corn oil. Ten additional 1 hr samples were taken for each animal. At the conclusion of the experiment, animals were perfused and probe placement was verified. Microdialysis samples were analyzed the same day by ELISA.

To determine Aβ half-life, time points between drug delivery and when Aβ concentrations plateaued were analyzed. For first-order processes, the elimination rate of a molecule from the body is directly related to the slope of the semi-log plot of concentration versus time: $a = -K_e/2.3$, where a represents the slope, and K_e represents the elimination rate constant. The half-life ($t_{1/2}$) of a molecule is the time necessary for the concentration to decrease by 50%. By definition of a first-order process, the half-life remains constant regardless of molecule concentration. The half-life can be expressed in terms of the elimination rate constant: $t_{1/2} = 0.693/K_e$.

APP Western. Tissue from 3-month-old PDAPP mice was harvested 8 hr after a 3 mg/kg subcutaneous injection of LY41175 or vehicle (corn oil). Animals were perfused with chilled PBS–heparin, and brains were dissected to isolate the hippocampus. Hippocampus was homogenized in radioimmunoprecipitation assay buffer (150 mM NaCl, 50 mM Tris, 0.5% deoxycholic acid, 1% Triton X-100, 0.1% SDS, 2.5 mM EDTA, and protease inhibitors, pH 8.0), and 40 μg of protein was loaded per lane of a reducing 10–20% Tris–tricine–SDS mini-gel. Proteins were separated at 80 mV and transferred to nitrocellulose. To detect APP C-terminal fragments (CTFs), the blot was probed with CT15 (a kind gift from Dr. Ed Koo, University of California, San Diego, La Jolla, CA), a rabbit polyclonal antibody against the terminal 15 amino acids of APP (Sisodia et al., 1993), followed by goat anti-rabbit HRP (Bio-Rad, Hercules, CA). To detect full-length APP, 6E10 (Signet Labs, Dedham, MA) was used, followed by sheep anti-mouse peroxidase (Amersham Biosciences). Signal was detected with SuperSignal West Pico Chemiluminescence (Pierce).

LY411575 brain exposure. Three- and 12-month-old PDAPP mice were injected subcutaneously with 3 mg/kg LY411575 in corn oil. Fifteen minutes after treatment, animals received a cardiac bleed and were immediately perfused with chilled PBS–heparin. Brains were removed and frozen at −80°C. Tissue was homogenized in acetonitrile (5:1 vol/gm wet weight), followed by C8 Empore solid phase extraction (3M, St. Paul, MN), and then analyzed for LY411575 content by liquid chromatography-tandem mass spectrometry similar to that described previously (Dovey et al., 2001).

Results

Characterization of Aβ in human CSF using *in vitro* microdialysis

Microdialysis has been useful in dynamically assessing the concentration of a variety of molecules in the brain ISF and has provided insight into their metabolism (Benveniste, 1989; Benveniste and Huttemeier, 1990). Because the concentration of brain ISF Aβ is likely to be an important, dynamically regulated pool of Aβ that determines whether Aβ aggregates, we began studies to determine whether ISF Aβ could be measured. To address this issue, we first began Aβ microdialysis studies *in vitro*. There are likely different forms of Aβ present in any solution, some percentage of which will be of appropriate size to cross the microdialysis membrane (Fig. 1*A*). We refer to Aβ that is measurable by microdialysis as exchangeable Aβ (eAβ). eAβ is a component of the total soluble Aβ within a sample that can diffuse across a 35 kDa membrane on the probe. Aβ bound to extracellular matrix, cell membrane, and large proteins, as well as some multimeric forms of Aβ, would be excluded.

During microdialysis, the perfusion buffer in the probe is flowing at a defined rate. Thus, molecules in the external solution do not have sufficient time to reach equilibrium with the internal dialysate buffer. The result is that the concentration of Aβ, and other molecules, in the collected microdialysis sample are a fraction of the measurable Aβ in solution. If experimental conditions remain the same, then the percentage of the target molecule recovered within the dialysate buffer will remain constant between samples. Once determined, the percentage recovery coefficient can then be applied to all samples collected under identical conditions.

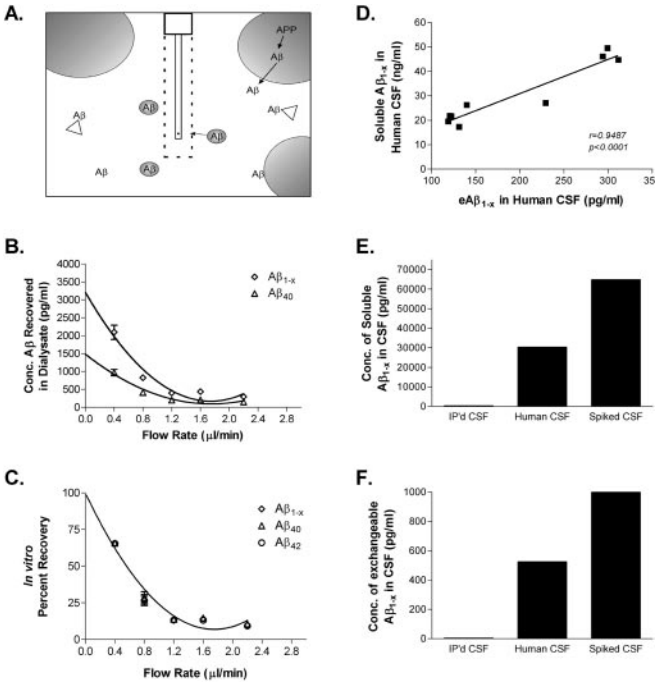

Figure 1. *In vitro* microdialysis to measure Aβ. *A*, Diagram of exchangeable Aβ. Triangles represent potential Aβ binding molecules, e.g., apoE, clusterin, and α2M. Only highlighted Aβ molecules are of the appropriate size to pass through a 35 kDA MWCO membrane on the microdialysis probe. *B*, Interpolated zero flow method to quantify the pool of measurable $Aβ_{1-x}$ and $Aβ_{40}$ within samples of human CSF ($n = 4$). At 2.2 μl/min, the percentage recovery of eAβ was 9.74 ± 1.53% (mean ± SEM). *C*, *In vitro* percentage recoveries for each Aβ species using the interpolated zero flow method. Each recovery point contains error bars and are overlapping for each species ($n = 4$). *In vitro* recovery of each Aβ species by microdialysis is the same. *D*, The concentration of eAβ and total soluble Aβ are highly correlated within a sample of human CSF (Pearson's $r = 0.9487$; $p < 0.0001$; $n = 9$). The mean concentrations of soluble $Aβ_{1-x}$ and $eAβ_{1-x}$ were 30.47 ± 4.23 ng/ml (mean ± SEM) and 196.2 ± 28.65pg/ml, respectively. *E*, *F*, Human CSF immunoprecipitated (IP'd) for Aβ has undetectable levels of total soluble Aβ and eAβ. Human CSF spiked with an amount of exogenous $Aβ_{40}$ peptide expected to double Aβ concentration resulted in a 2.1-fold increase in total soluble Aβ and a 1.9-fold increase in eAβ.

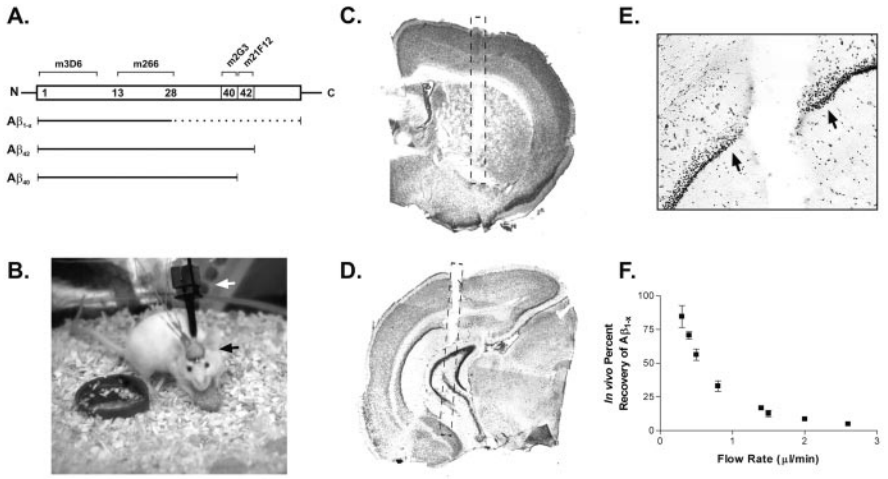

Figure 2. Aβ ELISA and *in vivo* microdialysis technique. *A*, Aβ species detected by ELISA for human $A\beta_{1\text{-}x}$, $A\beta_{40}$, and $A\beta_{42}$. Top, Aβ peptide sequence with epitopes recognized by each monoclonal (m) antibody. Bottom, Aβ species detected by each ELISA assay; solid lines represent segments of peptide that must be present for detection, and dashed lines represent segments of peptide that may vary but will still be recognized by the various antibody combinations. *B*, Awake mouse implanted with dual microdialysis probes. Black arrow denotes guide cannula–probe assembly; white arrow denotes collar used to attach mouse to balance arm that prevents force from being applied to implanted assembly. *C*, *D*, Representative probe placements in the hippocampus and striatum, respectively. Note partial probe tracts within each section. Hashed line depicts probe location. *D*, Cresyl violet stain of tissue surrounding the microdialysis probe tract after 18 hr implantation. There is no morphological evidence of substantial gliosis or inflammation along the tract (arrows), nor is there evidence of neuronal degeneration within the dentate granule cells. *F*, *In vivo* percentage recovery at various flow rates as determined by the interpolated zero flow method. At 0.5 and 2.6 μl/min, the percentage recovery of eAβ is 56.3 ± 4.21 and 4.9 ± 0.90% ($n = 4$), respectively.

To determine the *in vitro* percentage recovery of Aβ within samples of human CSF, we used two techniques: the interpolated zero flow and interpolated zero flux methods (Jacobson et al., 1985; Menacherry et al., 1992). The zero flow method varies the flow rate of perfusion buffer. By varying the flow rates, a recovery curve can be plotted with extrapolation back to a theoretical zero flow rate that represents perfect recovery from the target solution. The mean *in vitro* percentage recovery of eAβ at 2.2 μl/min using the zero flow method was ~10% at room temperature (Fig. 1*B*). The *in vitro* recoveries for $eA\beta_{1\text{-}x}$, $eA\beta_{40}$, and $eA\beta_{42}$ were the same at all flow rates (Fig. 1*C*). The zero flux method varies the concentration of Aβ within the microdialysis probe to assess at which concentrations Aβ diffuses into or out of the membrane. Using this method, we obtained similar percentage recoveries as the zero flow method (data not shown).

To characterize the exchangeable pool of Aβ in CSF, we determined the concentration of eAβ within individual samples of human CSF using the interpolated zero flow method and compared that with the concentration of total soluble Aβ present in the samples as measured directly by ELISA (Fig. 1*D*). In a series of human CSF samples, the mean concentration of soluble $A\beta_{1\text{-}x}$ was higher than the concentration of eAβ. Although eAβ was substantially lower than the total amount of soluble Aβ in the CSF, values of eAβ and total soluble Aβ were highly correlated (Fig. 1*D*). This suggests that, although the absolute concentration of soluble Aβ differs from eAβ, the concentrations of eAβ and soluble Aβ are directly proportional within human CSF under steady-state conditions. The reason that eAβ differs from measured soluble Aβ is likely attributable to Aβ-binding molecules that hinder the diffusion of ~4 kDa Aβ across the 35 kDa dialysis membrane. Potential candidate Aβ-binding molecules include apolipoprotein E (Yang et al., 1997), α-2-macroglobulin (Du et al., 1997), and clusterin (Ghiso et al., 1993; Matsubara et al., 1995), among others.

To further assess whether the concentration of eAβ directly reflects the concentration of total soluble Aβ within a physiological sample, the concentration of eAβ was measured by *in vitro* microdialysis in a normal sample of human CSF, as well as in identical samples in which (1) Aβ was removed by immunoprecipitation or (2) CSF Aβ concentration was increased by adding exogenous $A\beta_{40}$. This simulated an acute decrease or increase of Aβ within that sample. Values for soluble Aβ were assessed directly by ELISA in CSF (Fig. 1*E*), and eAβ in the same sample was assessed by microdialysis followed by ELISA (Fig. 1*F*). CSF in which Aβ was immunoprecipitated had virtually no detectable total soluble Aβ or eAβ. CSF spiked with exogenous $A\beta_{40}$ (with an amount of Aβ expected to be double the normal concentration) had twofold higher levels of both soluble Aβ and eAβ. Thus, the concentration of eAβ directly reflects the concentration of soluble Aβ under steady-state conditions, as well as after a sudden change.

Species of Aβ analyzed

Because our various ELISA assays use monoclonal antibodies that recognize particular Aβ epitopes, we were able to measure specific Aβ species (Fig. 2*A*). The $A\beta_{1\text{-}x}$ ELISA is a measurement of all Aβ from amino acid 1 to amino acid 28 or greater. The $A\beta_{40}$ and $A\beta_{42}$ ELISA recognizes full-length Aβ from amino acid 1 to either 40 or 42. As a result, a subtraction of the concentration of $A\beta_{40}$ and $A\beta_{42}$ from $A\beta_{1\text{-}x}$ yields any Aβ species in which the N terminus begins at position 1 and has a C terminus that does not end in position 40 or 42. These Aβ C-terminal variants could include $A\beta_{1-38}$, $A\beta_{1-39}$, and $A\beta_{1-43}$.

Characterization of *in vivo* microdialysis technique

After validation of eAβ measurement using *in vitro* microdialysis (Fig. 1), we initiated an *in vivo* assessment of ISF eAβ in PDAPP mice. Microdialysis probes were implanted stereotactically under anesthesia. Figure 2, *C* and *D*, depicts representative probe placements in the hippocampus and striatum. The animals were permitted to awaken from the anesthetic and remained awake for the duration of the experiment (Fig. 2*D*).

Although insertion of a microdialysis probe does cause some acute and/or chronic injury to the surrounding tissue, we took measures to minimize this effect on our experiments. During probe insertion, there is some acute tissue injury, and the blood–brain barrier (BBB) integrity is compromised. However, the BBB has been shown to be rapidly repaired, and it progressively excludes smaller molecules as tight junctions reform. Small molecules, such as sucrose, are impermeable to the BBB within 3–4 after microdialysis probe implantation (Dykstra et al., 1992), whereas it only takes 30 min for larger molecules, such as Evan's blue (molecular weight of 960) (Morgan et al., 1996), to be impermeable. Chronic changes can include astrogliosis and inflammatory processes. These changes usually begin 24–36 hr after probe insertion and may effect long-term implantations by changing the local environment that the microdialysis probe membrane contacts. We limited our experimental window to

hours 4–18 after probe insertion so there is time after the initial injury for the BBB to exclude large molecules; however, the experiment concludes before substantial chronic processes have occurred.

As assessed by cresyl violet staining (Fig. 2*E*), tissue surrounding a microdialysis probe implanted for 18 hr shows some tissue displacement, but, in the area immediately adjacent to the probe, neurons are intact and there is no marked glial activation. This was confirmed by the absence of an increase in GFAP staining (data not shown). We also found no evidence of activated caspase-3 immunostaining in any of the tissue analyzed, nor was there evidence of local Aβ accumulation or removal as a result of probe insertion (data not shown). In PDAPP animals implanted with microdialysis probes for 18 hr (longest time point) that were given no other manipulations, the ISF eAβ concentration after 18 hr was not significantly different from the baseline concentration (mean concentration for hours 4–8), suggesting that these limited environmental changes did not adversely effect the ISF eAβ concentration in these experiments.

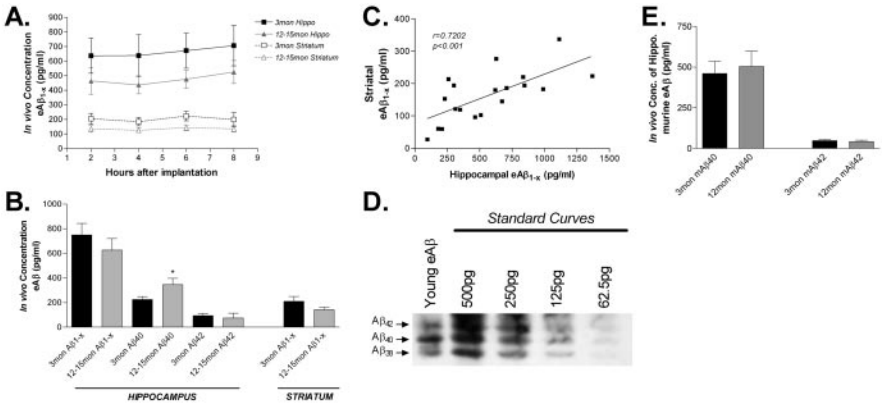

Figure 3. *In vivo* concentration of eAβ in young and middle-aged PDAPP mice. *A*, ISF eAβ concentrations in hippocampus and striatum of 3- and 12- to 15-month-old PDAPP mice. Three-month-old mice have 727.7 ± 92.1 pg/ml ($n = 21$; mean ± SEM) and 207.9 ± 31.8 pg/ml ($n = 6$) of $eA\beta_{1\text{-}x}$ in the hippocampus and striatum, respectively. Twelve- to 15-month-old mice have 626.4 ± 93.3 pg/ml ($n = 21$) and 142.1 ± 19.5 pg/ml ($n = 13$) of eAβ in those regions. *B*, The concentration of eAβ species in young and aged mice. The concentration of $eA\beta_{1\text{-}x}$ does not change significantly with age. $eA\beta_{40}$ increases significantly in the hippocampus with age ($p = 0.0429$), whereas $eA\beta_{42}$ does not decrease ($p = 0.6116$). *C*, The concentration of $eA\beta_{1\text{-}x}$ within the hippocampus and striatum are highly correlated (Pearson's $r = 0.7202$; $p < 0.001$; $n = 19$). *D*, A microdialysis sample was analyzed by acid–urea electrophoresis, followed by Western blot analysis to visualize the various Aβ species present. On the basis of the peptide standard curves, $A\beta_{42}$, $A\beta_{40}$, and $A\beta_{38}$ represent 15.6, 31.6, and 52.8%, respectively, of the ISF Aβ detected. No other Aβ species were detected. This confirms that Aβ-CTV is a major pool of Aβ in the ISF and that $A\beta_{38}$ is the predominant species. *E*, The concentration of endogenous murine ISF $eA\beta_{40}$ and $eA\beta_{42}$ was measured in 3-month-old ($n = 6$) and 12-month-old ($n = 6$) C57BL/6 mice. There was no change with age in the concentration of murine $eA\beta_{40}$ ($p = 0.718$) or $eA\beta_{42}$ ($p = 0.609$) in wild-type mice.

In vivo measurement of interstitial fluid Aβ in PDAPP mice

The *in vivo* percentage recovery of eAβ for both 3- and 12- to 15-month-old PDAPP mice were the same (Fig. 2*F*), as was the recovery of $eA\beta_{1\text{-}x}$, $eA\beta_{40}$, and $eA\beta_{42}$ (data not shown). The recovery coefficients at each flow rate were applied to the Aβ concentration obtained in dialysate samples to calculate the actual *in vivo* concentration of eAβ. The percentage recovery between 3- and 12- to 15-month-old mice did not differ significantly ($p = 0.769$; repeated-measures ANOVA with Huynh and Feldt adjustment).

To assess the baseline concentration of regional eAβ, microdialysis probes were implanted into the hippocampus and striatum of 3- and 12- to 15-month-old animals, 2 hr fractions of dialysis buffer were collected over a period of 8–12 hr, and $A\beta_{1\text{-}x}$ was measured by ELISA (Fig. 3*A*). The value of ISF eAβ for a given animal was determined by taking the mean concentration of the sample fractions from hours 5–8 to control for slight variations between time points. Measurements of ISF eAβ for up to 18 hr after probe implantation were stable. Three-month-old PDAPP animals, which have not developed Aβ deposits as plaques, had an $eA\beta_{1\text{-}x}$ concentration in the hippocampus and striatum of ~730 and 210 pg/ml, respectively (for actual Aβ values, seeTable 1). The hippocampus and striatum of 12- to 15-month-old mice with Aβ deposition had $eA\beta_{1\text{-}x}$ concentrations of 630 and 140 pg/ml, respectively. Regional $eA\beta_{1\text{-}x}$ did not differ significantly between age groups ($p = 0.6244$); however, there was a trend for older mice (which have Aβ deposits) to have a lower concentration of $eA\beta_{1\text{-}x}$ in the striatum ($p = 0.0839$). Although the mean concentration of hippocampal $eA\beta_{1\text{-}x}$ was lower in older mice, this difference was not significant ($p = 0.4457$). The ratio of hippocampal to striatal $eA\beta_{1\text{-}x}$ in both 3-month-old and 12- to 15-month-old animals was 3.5:1, which is similar to the ratios of $A\beta_{1\text{-}x}$ in brain lysates of these regions (ratio of 5.3:1; data not shown). The concentration of ISF $eA\beta_{1\text{-}x}$ within the hippocampus and striatum of both age groups correlated significantly (Fig. 3*C*).

In a subset of 3- and 12- to 15-month-old mice, the hippocampal mean $eA\beta_{40}$ and $eA\beta_{42}$ concentrations were also determined using a microdialysis protocol with a slower flow rate designed to enrich the samples for Aβ to facilitate measurement. The concentration of hippocampal $eA\beta_{40}$ in 3-month-old and 12- to 15-month-old PDAPP was ~220 pg/ml ($n = 6$) and 350 pg/ml ($n = 4$) respectively, whereas $eA\beta_{42}$ was 95 pg/ml ($n = 6$) and 75 pg/ml ($n = 4$) respectively. Although hippocampal $eA\beta_{1\text{-}x}$ values did not differ between age groups, the concentration of $eA\beta_{40}$ increased significantly in 12- to 15-month-old mice ($p = 0.0429$), whereas $eA\beta_{42}$ levels did not change with age ($p = 0.6116$). Together, this suggests that Aβ C-terminal variants ($A\beta_{1\text{–}38}$, $A\beta_{1\text{–}39}$, and $A\beta_{1\text{–}43}$) were likely decreasing in older mice. To confirm that Aβ C-terminal variants are present in ISF and to determine the major species within that pool, we performed acid–urea gel analysis, followed by Western blotting of eAβ from a microdialysis sample. This revealed that $A\beta_{38}$ is the major Aβ C-terminal variant present in ISF in 3-month-old (Fig. 3*D*) and 12- to 15-month-old mice (data not shown). $A\beta_{38}$ has been shown previously to be a major Aβ species in brain and CSF, as well (Weggen et al., 2001; Wiltfang et al., 2002; Pype et al., 2003).

ISF murine $A\beta_{40}$ and $A\beta_{42}$ was also measured by microdialysis in 3- and 12-month-old wild-type mice (C57BL/6). The concentrations of murine $eA\beta_{40}$ and $eA\beta_{42}$ were not altered between the groups (Fig. 3*E*). That murine eAβ does not change with age and previous findings that human Aβ production does not change with age in PDAPP mice (Johnson-Wood et al., 1997) suggest that the changes in Aβ species between young and middle-aged PDAPP mice are not age related but instead are related to Aβ deposition.

Table 1. Concentrations of Aβ in the ISF, CSF, and tissue lysates in young and aged mice

	Mean ± SEM concentration					
	3 months			12–15 months		
Tissue–fluid	$A\beta_{1-x}$	$A\beta_{40}$	$A\beta_{42}$	$A\beta_{1-x}$	$A\beta_{40}$	$A\beta_{42}$
ISF–hippo (pg/ml)	727.7 ± 92.1	224.4 ± 23.3	93.6 ± 16.9	626.4 ± 93.9	345.9 ± 52.2	73.9 ± 38.9
ISF–striatum (pg/ml)	207.1 ± 31.8			142.1 ± 19.5		
CSF (pg/ml)	11337 ± 699.7	5058 ± 496.0	2375 ± 336.8	8451 ± 915.3	4272 ± 898.7	961 ± 170.0
Hippo–carbonate (pg/mg protein)	255.0 ± 42.9	70.1 ± 14.5	80.3 ± 15.4	1147.6 ± 383.7	93.2 ± 29.7	692.5 ± 194.9
Hippo–guanidine (pg/mg protein)	1126 ± 135.9	105 ± 21.7	291 ± 30.4	87476 ± 29714	8159 ± 2775	66214 ± 22315

The concentration of ISF eAβ was assessed by microdialysis ($n = 21$). CSF was isolated from the cisterna magna and directly analyzed by ELISA ($n = 6$). Hippocampal tissues were processed by sequential extraction in carbonate buffer and then 5 M guanidine ($n = 6$). Tissue Aβ values are normalized to protein concentrations for each sample. Hippo, Hippocampus.

Relationship between ISF eAβ and tissue Aβ

$A\beta_{40}$ and $A\beta_{42}$ levels in CSF and tissue were also assessed in 3-month-old and 12- to 15-month-old animals (Table 1). Similar to previously published results (DeMattos et al., 2002b), CSF $A\beta_{42}$ levels decreased significantly with age ($p = 0.0266$), whereas in hippocampal brain lysates, carbonate and guanidine extractable $A\beta_{42}$ levels markedly increased (4.5-fold and 78-fold; $p = 0.0043$ and $p = 0.0057$, respectively). The carbonate buffer used is an alkaline, nondenaturing buffer, whereas guanidine is a chaotropic, denaturing buffer that solubilizes most, if not all, of the Aβ aggregates. The increase in soluble Aβ in tissue lysates (e.g., carbonate) subsequent to plaque formation has been interpreted by some as an increase in extracellular, soluble Aβ in the brain that may contribute to its toxicity. However, in contrast to the increased concentration of soluble $A\beta_{42}$ in tissue lysates with age, the concentration of $A\beta_{42}$ in ISF does not significantly change with age or the presence of Aβ deposits. This suggests that much of the soluble Aβ in tissue lysates may not be truly "soluble" and diffusible in the extracellular space. Much of this tissue-soluble pool is likely intracellular, associated with membranes, or loosely associated to Aβ aggregates. Thus, we conclude that soluble Aβ in the brain lysate, in the presence of plaques, does not reflect soluble ISF eAβ.

To further compare Aβ metabolism between different brain compartments, we compared the ratios of $A\beta_{40}/A\beta_{42}$ in ISF, CSF, and brain lysates. In both ISF and CSF, the $A\beta_{40}/A\beta_{42}$ ratio significantly increased in 12- to 15-month-old animals (Fig. 4). Interestingly, this increased ratio in ISF is attributable to an increase in $A\beta_{40}$, whereas in CSF, it is attributable to a decrease in $A\beta_{42}$. In contrast, in 12- to 15-month-old PDAPP mice, carbonate and guanidine extracted tissue lysates had a markedly decreased $A\beta_{40}/A\beta_{42}$ ratio, primarily attributable to a tremendous increase in aggregated $A\beta_{42}$. That $A\beta_{40}$ and $A\beta_{42}$ are changing in different patterns in ISF, CSF, and tissue underscores the difference in metabolism among these three compartments.

Relationships between ISF Aβ, CSF Aβ, and plaque load

To determine how various pools of CNS Aβ are related, a variety of samples were collected from a cohort of mice. Aβ values were determined in hippocampal ISF, CSF, and soluble and insoluble hippocampal tissue lysates. For each of these samples, $A\beta_{1-x}$, $A\beta_{40}$, and $A\beta_{42}$ were analyzed. The amount of Aβ deposited in plaques in the hippocampus (percentage Aβ load) was also quantified. These results enabled us to analyze correlations between the various compartments of Aβ in individual mice (Fig. 5). In 3-month-old PDAPP mice, there was no correlation between ISF and CSF Aβ levels (Fig. 5*A*), suggesting that, in the absence of insoluble Aβ in plaques, Aβ levels in these pools are independent. In contrast to these findings, there was a significant correlation between ISF and CSF Aβ levels in 12- to 15-month-old mice (Fig. 5*B*). All of the mice at this age have biochemical or pathological (plaques) evidence of Aβ aggregation, suggesting that the presence of insoluble Aβ is either associated with, or directly causes, a change in ISF or CSF Aβ metabolism, resulting in a new equilibrium between ISF eAβ, CSF Aβ, and deposited insoluble Aβ. In 12- to 15-month-old PDAPP mice, there was a significant correlation between the concentration of CSF $A\beta_{1-x}$ and Aβ plaque load (Fig. 5*C*) as noted previously (DeMattos et al., 2002b). There was also a trend for the hippocampal ISF Aβ and Aβ load to correlate (Fig. 5*D*). This suggests that the pool of aggregated, insoluble Aβ directly influences two distinct pools of soluble, extracellular Aβ.

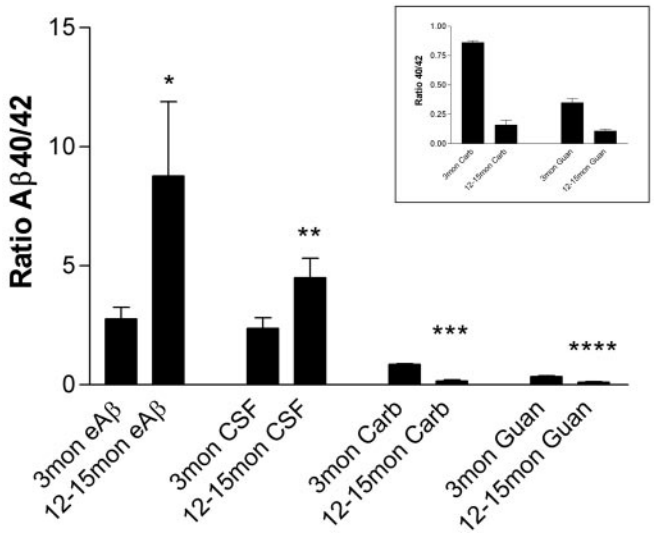

Figure 4. Differences in $A\beta_{40}/A\beta_{42}$ ratios between ISF, CSF, and brain tissue with age. In both the ISF and CSF fluids, the $A\beta_{40}/A\beta_{42}$ ratio increases significantly with age ($p = 0.0466$, $n = 10$; and $p = 0.0413$, $n = 9$, respectively), primarily attributable to an increase in $A\beta_{40}$ within ISF and a decrease in $A\beta_{42}$ in CSF. In contrast, carbonate (Carb) and guanidine (Guan) of hippocampal tissue reveals a significant decrease in the $A\beta_{40}/A\beta_{42}$ ratio with age ($p < 0.0001$ and $p < 0.001$, respectively; $n = 10$). This change coincides with a tremendous deposition of $A\beta_{42}$ in older mice. Inset, Enlargement of hippocampal tissue lysate data.

Half-life of Aβ in the brain interstitial fluid

It has been speculated for some time that the accumulation of both soluble and insoluble Aβ in a β-sheet conformation (e.g., oligomers and fibrils) in the brain may alter the metabolism of Aβ in the other soluble pools within the CNS. One way to directly assess this issue is to determine the *in vivo* half-life of different pools of Aβ in mice with or without Aβ aggregates. Because *in vivo* microdialysis allows for a dynamic assessment of the interstitial fluid space, we estimated the *in vivo* $t_{1/2}$ of ISF $eA\beta_{1-x}$ after

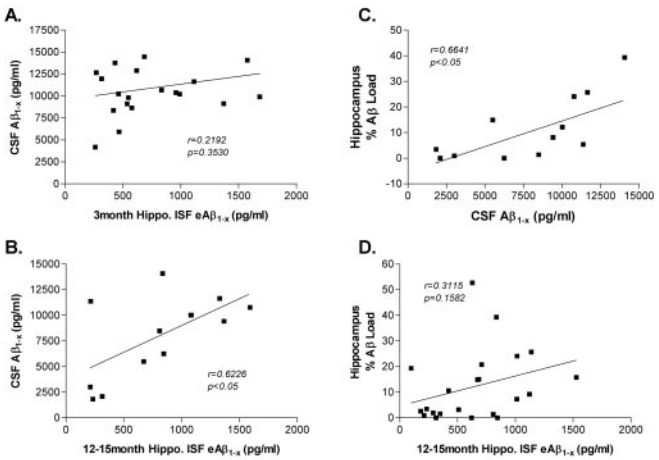

Figure 5. Relationship of Aβ between CNS compartments. *A*, There is no correlation between CSF Aβ and hippocampal (Hippo.) ISF eAβ in 3-month-old PDAPP mice (Pearson's $r = 0.2192$; $p = 0.3530$; $n = 20$). *B*, In 12- to 15-month-old PDAPP mice, there is a significant correlation between CSF Aβ and hippocampal ISF eAβ (Pearson's $r = 0.6226$; $p = 0.023$; $n = 13$). In middle-aged mice, there is a significant correlation between CSF Aβ and percentage Aβ load (*C*) (Pearson's $r = 0.6641$; $p = 0.0133$; $n = 13$), as well as a positive trend between ISF eAβ and percentage Aβ load in the hippocampus (*D*) (Pearson's $r = 0.3511$; $p = 0.1582$; $n = 22$).

rapid inhibition of Aβ production via a potent γ-secretase inhibitor.

Microdialysis probes were implanted into the hippocampus of 3-month-old or 12-month-old PDAPP mice. For each animal, the baseline concentration of ISF eAβ was determined by taking eight 1 hr microdialysis samples. At the end of hour 8, a potent, brain-penetrant γ-secretase inhibitor, LY411575 (Wu et al., 1998), was injected subcutaneously. Ten additional 1 hr samples were taken after treatment with either the drug or vehicle (corn oil). Within the first hour of treatment, both age groups had decreased concentrations of $eA\beta_{1\text{-}x}$. In 3- and 12-month-old animals, eAβ levels reached ~20% of baseline by 6 hr after treatment (Fig. 6*A*). There was no significant difference in the new baseline Aβ concentrations after treatment between the two age groups. Interestingly, the $t_{1/2}$ of ISF Aβ after LY411575 treatment was markedly different between young and middle-aged mice ($p = 0.0045$). Analysis of the $t_{1/2}$ for eAβ in the hippocampal ISF was 1.97 ± 0.623 hr in young mice and 3.78 ± 0.866 hr in aged mice (Fig. 6*B*). A semi-log plot of baseline concentration versus time was linear at both ages (Fig. 6*B*), suggesting first-order kinetics for Aβ metabolism within the brain interstitial fluid. ISF eAβ levels in vehicle-injected, 3- and 12-month-old mice remained relatively steady for the 18 hr of microdialysis and did not vary dramatically after injection at hour 9 (Fig. 6*A*).

LY411575 reaches peak concentrations in the brain ~15 min after a 3 mg/kg subcutaneous injection. In 15 min, we found that brain levels of LY411575 were ~200-fold in excess of the IC_{50} necessary in cell lines for γ-secretase inhibition (data not shown), and drug entry into the brain was equal in both 3- and 12-month-old PDAPP mice (Fig. 6*C*). As expected, a Western blot for APP C-terminal fragments in hippocampal tissue at the end of the experiment showed an increase in β-CTF and α-CTF, consistent with the γ-secretase cleavage being inhibited by LY411575 (Fig. 6*D*). The amount of full-length APP did not change in response to treatment. Together, these results not only demonstrate the remarkably short half-life of ISF eAβ, but that, concomitant with the formation of Aβ aggregates, there is a marked change in ISF eAβ metabolism that becomes apparent once synthesis is blocked.

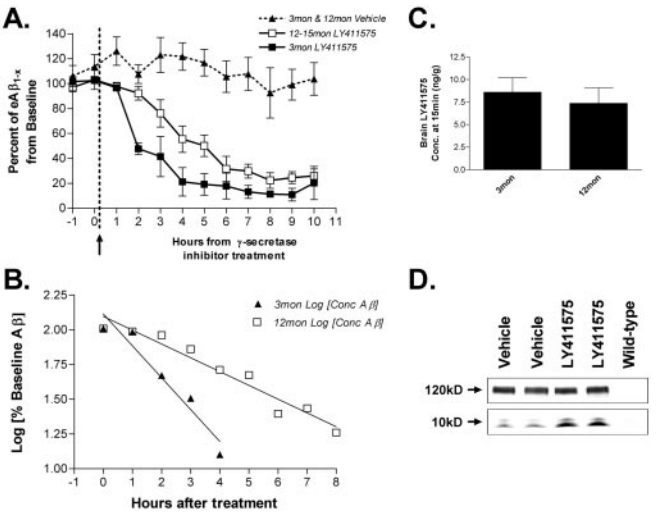

Figure 6. Half-life of ISF eAβ in young and middle-aged PDAPP mice. *A*, Effect of LY411575 on hippocampal $eA\beta_{1\text{-}x}$ concentration in 3- and 12-month-old PDAPP mice. During microdialysis, animals received a 3 mg/kg subcutaneous injection of LY411575 or vehicle (corn oil). Concentrations of $eA\beta_{1\text{-}x}$ dropped to 21.16 ± 11.46% (mean ± SEM; $n = 4$) and 22.34 ± 6.23% ($n = 5$) of baseline by 4 and 8 hr in young and middle-aged mice, respectively ($p = 0.0045$; repeated-measures ANOVA with Huynh and Feldt adjustment). Three-month-old ($n = 5$) and 12-month-old ($n = 4$) vehicle-injected mice do not show a significant change in Aβ concentration after treatment. *B*, A semi-log plot of percentage baseline of eAβ versus time is linear (young, $y = -0.229x + 2.11$, $r^2 = 0.936$; middle-aged, $y = -0.099 + 2.10$, $r^2 = 0.9173$), suggesting first-order kinetics of Aβ elimination in both age groups. The half-life of Aβ within the ISF of young mice is 1.97 ± 0.623 hr ($n = 4$) and in aged mice is 3.78 ± 0.866 hr ($n = 5$). *C*, Concentration of LY411575 in whole brain of 3- and 12-month-old PDAPP mice 15 min after 3 mg/kg subcutaneous injection ($n = 6$). LY411575 enters the brain equally in both age groups with a concentration that was ~220-fold higher than the IC_{50} needed to inhibit γ-secretase activity in cell culture. *D*, A Western blot probed for full-length and C-terminal fragments of APP. Tissue samples are from 3-month-old PDAPP mice injected with 3 mg/kg LY411575 or vehicle and killed at 8 hr after treatment ($n = 8$). Full-length APP levels do not change between these groups (top panel); however, both α-CTF and β-CTF increased in LY411575-treated mice (bottom panel), as expected with γ-secretase cleavage inhibited.

Discussion

Brain ISF eAβ is likely the pool of Aβ that mediates its normal functions, if any, as well as being the major precursor to conformationally altered forms of Aβ in the brain (e.g., plaques and oligomers). This study demonstrates that soluble, ISF Aβ can be measured on a dynamic time scale, exclusive from the other CNS compartments. This provides a method to determine whether an acute manipulation to an individual animal alters an Aβ pool likely to be critical in AD pathogenesis. We demonstrated that the overall concentration of ISF $eA\beta_{1\text{-}x}$ does not change dramatically with age and Aβ deposition in PDAPP mice (Fig. 3). There is, however, a substantial change in Aβ metabolism associated with Aβ deposition, as evidenced by altered relationships between Aβ species (e.g., $A\beta_{40}$, $A\beta_{42}$, and Aβ C-terminal variants) and between CNS compartments. We also demonstrate that the *in vivo* half-life of ISF eAβ is short in 3-month-old animals (~2 hr). Importantly however, in 12- to 15-month-old PDAPP mice that have Aβ deposits, the apparent $t_{1/2}$ of ISF eAβ is doubled. This, coupled with previous *in vitro* studies (Maggio et al., 1992), strongly suggests that, in addition to a large amount of insoluble Aβ that is primarily immobile, that there is a pool of extracellular Aβ in dynamic equilibrium between soluble and insoluble forms of Aβ. This pool can be visualized with use of a γ-secretase inhibitor and appears to be associated, but not locked onto, fibrils (Fig. 7, see model). It is this mobile pool that appears to be revealed by inhibition of Aβ production. The ability to now assess the effects

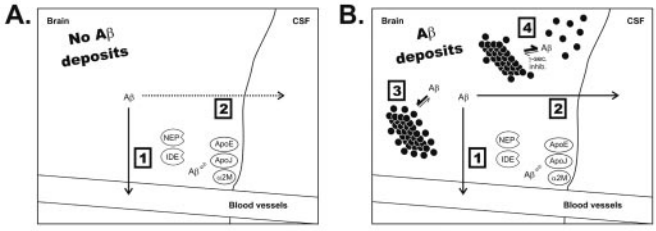

Figure 7. Proposed diagram of Aβ metabolism within the CNS in the presence and absence of Aβ deposits. Aβ appears to be cleared from the ISF by efflux out of the brain and by local degradation (*1*), as well as by ISF to CSF bulk flow and ISF to periphery bulk flow (*2*). *3*, Under normal conditions in the presence of deposits, the on-rate of Aβ into plaques is slow but faster than the off-rate, causing an accumulation onto Aβ plaques. *4*, In the presence of a γ-secretase inhibitor, a fraction of the insoluble docked Aβ can become soluble and reenter the interstitial fluid.

on ISF eAβ by endogenous molecules, as well as potential treatments such as Aβ-degrading enzymes (Iwata et al., 2000; Farris et al., 2003), Aβ-chelators (Cherny et al., 2001), and anti-Aβ antibodies, may provide a useful approach to understanding pathogenesis, as well as evaluating Aβ-related diagnostic and treatment strategies.

Altered Aβ metabolism with age and Aβ aggregation

The relative concentrations of hippocampal and striatal ISF eAβ mirror the levels of human APP expression and total tissue Aβ levels in young PDAPP mice. With Aβ conformational change, the concentration of ISF $eA\beta_{1-x}$ does not change dramatically; however, $eA\beta_{40}$ increased significantly, whereas $eA\beta_{42}$ did not change. This was accompanied by an apparent decrease in ISF Aβ C-terminal variants, which appear to consist predominantly of $A\beta_{38}$. Thus, age-related and, more likely, Aβ deposition-related alterations in ISF Aβ metabolism are Aβ species specific. Interestingly, the concentration of ISF $A\beta_{42}$ did not change with Aβ deposition. It has been postulated that the concentration of ISF Aβ would decrease as a consequence of aggregation. Aβ deposition, however, is a chronic process, and, at any given time, it is likely that the amount of newly synthesized $A\beta_{42}$ that becomes insoluble is a small percentage of the ongoing $A\beta_{42}$ produced and released into ISF. Thus, the small overall mass of depositing versus produced $A\beta_{42}$, at any given time, does not appear to be detectable in ISF under basal conditions.

ISF eAβ is a pool of Aβ distinct from CSF and soluble Aβ in tissue lysates. ISF eAβ reflects local Aβ production, release, degradation, and clearance, whereas CSF Aβ more likely reflects Aβ metabolism from the entire CNS, not a specific region. CSF production and removal also occurs via different pathways than ISF production and removal (Cserr et al., 1992; Zhang et al., 1992). Tissue lysates include all forms of extracellular and intracellular Aβ, including some Aβ that may be "loosely" associated with insoluble Aβ aggregates yet is soluble after tissue lysis, even in mild salt and alkaline buffers (Simmons et al., 1994). The clear demarcation between these compartments is evident by their differing ratios of $A\beta_{40}/A\beta_{42}$. Interestingly, with age and deposition, $A\beta_{40}/A\beta_{42}$ ratios change in distinct, yet different, patterns in each CNS compartment, in part because the individual Aβ species in each compartment are changing in different ways. For example, in 12- to 15-month-old versus 3-month-old PDAPP mice, both CSF $A\beta_{40}$ and $A\beta_{42}$ decrease; however, ISF $eA\beta_{40}$ increases. These changes in individual Aβ species suggest that there is a fundamental change in Aβ metabolism in PDAPP mice likely attributable to the presence of insoluble Aβ aggregates because changes in murine Aβ do not occur in age-matched wild-type mice.

Although Aβ levels within each CNS compartment are regulated in a particular manner, with Aβ conformational change, a new relationship between the ISF and CSF is observed. A significant correlation of Aβ levels emerges when comparing ISF and CSF in 12- to 15-month-old but not 3-month-old mice (Fig. 5). This suggests that, with time and deposition, a new equilibrium between ISF and CSF develops that does not exist in younger mice. ISF $A\beta_{1-x}$ concentration did not differ between young and middle-aged mice, suggesting no net change in Aβ elimination. However, it is conceivable that, in the presence of Aβ deposits, Aβ elimination from ISF involves not only local degradation, ISF clearance, and blood–brain barrier transport but also greater ISF to CSF transport than in younger mice.

Interstitial fluid Aβ half-life

Dynamic sampling via microdialysis enabled us to follow ISF eAβ concentrations in 3- and 12- to 15-month-old PDAPP mice before and after treatment with a potent γ-secretase inhibitor that rapidly blocks CNS Aβ production. The half-life for ISF eAβ in young mice is relatively short, ~2 hr. This short $t_{1/2}$ for ISF Aβ in young mice suggests that Aβ is rapidly and constantly produced, cleared, and replenished within the extracellular space. Intriguingly, in older mice with the appearance of Aβ aggregates, ISF eAβ has a significantly longer, twofold increase in half-life or elimination rate. Aβ production has been shown not to change in young versus older PDAPP mice (Johnson-Wood et al., 1997). Thus, inhibition of Aβ synthesis revealed a major difference in Aβ metabolism between young and middle-aged PDAPP mice that was not obvious under basal conditions. This extended half-life, however, does not correspond with an increased concentration of ISF $A\beta_{1-x}$. If the concentration of ISF $A\beta_{1-x}$ were increased, this would suggest a fundamental change in Aβ elimination via degradation, clearance, or both in young versus middle-aged mice. The absence of this increase in ISF $eA\beta_{1-x}$ suggests another explanation for the prolonged $t_{1/2}$ in old mice. The data show that, after inhibition of Aβ production in mice with Aβ deposits, the concentration of eAβ drops. As this occurs, it appears that the dynamic equilibrium between extracellular soluble and insoluble Aβ can be measured and uncovered. *In vitro* studies have shown that Aβ aggregates contain a readily dissociable pool of Aβ, or "docked Aβ," as well as a long-lasting or stable "locked" pool of Aβ (Maggio et al., 1992; Esler et al., 2000). *In vitro*, as the concentration of Aβ in solution decreases, this docked pool can quickly dissociate from fibrils. *In vivo*, when Aβ production is inhibited and ISF Aβ levels begin to decrease, it is likely that this associated, docked pool can return to solution over a finite period of time, as occurs *in vitro*, causing this pool of Aβ to dissociate from fibrils and become soluble. This would result in a prolonged apparent half-life of ISF Aβ in animals with Aβ deposition.

Model of Aβ-aggregation induced changes in Aβ metabolism *in vivo*

We propose that, in the absence of Aβ deposition in the brain, Aβ is readily cleared from the interstitial fluid by several mechanisms (Fig. 7) (Cserr et al., 1992; Iwata et al., 2000; Shibata et al., 2000; Farris et al., 2003). We postulate that an alteration in Aβ metabolism, probably related to the presence of Aβ deposits, leads to changes in the equilibrium of different Aβ species within brain compartments. This change in equilibrium results in a new correlation between some of these compartments. When Aβ pro-

duction is inhibited, we hypothesize that a new equilibrium is established between ISF Aβ and a loosely associated pool of docked, deposited Aβ that can reenter the soluble eAβ pool. This docked pool may represent conformationally altered forms of Aβ, such as protofibrils (Hartley et al., 1999; Walsh et al., 1999) and oligomers (Kayed et al., 2003), that have been shown *in vitro* and after injection *in vivo* (Walsh et al., 2002) to be extremely toxic. If so, inhibition of Aβ production with γ-secretase inhibitions may rapidly decrease this toxic pool. From a diagnostic standpoint, the presence of this docked pool may also be very important. It appears that Aβ aggregation and plaques begin to build up in the human brain ~10–20 years before the onset of clinical symptoms of AD (preclinical AD) (Morris and Price, 2001). Therefore, if visualization of this prolonged $t_{1/2}$ in the presence of Aβ aggregates can be assessed in humans (for example via assessment of plasma Aβ) (DeMattos et al., 2002a), it may provide a novel, non-invasive method to detect the presence of Aβ aggregation and deposition *in vivo*.

References

Bales KR, Verina T, Dodel RC, Du Y, Altstiel L, Bender M, Hyslop P, Johnstone EM, Little SP, Cummins DJ, Piccardo P, Ghetti B, Paul SM (1997) Lack of apolipoprotein E dramatically reduces amyloid beta-peptide deposition. Nat Genet 17:263–264.

Benveniste H (1989) Brain microdialysis. J Neurochem 52:1667–1679.

Benveniste H, Huttemeier PC (1990) Microdialysis—theory and application. Prog Neurobiol 35:195–215.

Cherny RA, Atwood CS, Xilinas ME, Gray DN, Jones WD, McLean CA, Barnham KJ, Volitakis I, Fraser FW, Kim Y, Huang X, Goldstein LE, Moir RD, Lim JT, Beyreuther K, Zheng H, Tanzi RE, Masters CL, Bush AI (2001) Treatment with a copper-zinc chelator markedly and rapidly inhibits beta-amyloid accumulation in Alzheimer's disease transgenic mice. Neuron 30:665–676.

Cserr HF, Harling-Berg CJ, Knopf PM (1992) Drainage of brain extracellular fluid into blood and deep cervical lymph and its immunological significance. Brain Pathol 2:269–276.

DeMattos RB, Bales KR, Cummins DJ, Dodart JC, Paul SM, Holtzman DM (2001) Peripheral anti-A beta antibody alters CNS and plasma A beta clearance and decreases brain A beta burden in a mouse model of Alzheimer's disease. Proc Natl Acad Sci USA 98:8850–8855.

DeMattos RB, Bales KR, Cummins DJ, Paul SM, Holtzman DM (2002a) Brain to plasma amyloid-beta efflux: a measure of brain amyloid burden in a mouse model of Alzheimer's disease. Science 295:2264–2267.

DeMattos RB, Bales KR, Parsadanian M, O'Dell MA, Foss EM, Paul SM, Holtzman DM (2002b) Plaque-associated disruption of CSF and plasma amyloid-beta (Abeta) equilibrium in a mouse model of Alzheimer's disease. J Neurochem 81:229–236.

DeMattos RB, O'Dell MA, Parsadanian M, Taylor JW, Harmony JA, Bales KR, Paul SM, Aronow BJ, Holtzman DM (2002c) Clusterin promotes amyloid plaque formation and is critical for neuritic toxicity in a mouse model of Alzheimer's disease. Proc Natl Acad Sci USA 99:10843–10848.

Dovey HF, John V, Anderson JP, Chen LZ, de Saint Andrieu P, Fang LY, Freedman SB, Folmer B, Goldbach E, Holsztynska EJ, Hu KL, Johnson-Wood KL, Kennedy SL, Kholodenko D, Knops JE, Latimer LH, Lee M, Liao Z, Lieberburg IM, Motter RN, et al. (2001) Functional gamma-secretase inhibitors reduce beta-amyloid peptide levels in brain. J Neurochem 76:173–181.

Du Y, Ni B, Glinn M, Dodel RC, Bales KR, Zhang Z, Hyslop PA, Paul SM (1997) alpha2-Macroglobulin as a beta-amyloid peptide-binding plasma protein. J Neurochem 69:299–305.

Dykstra KH, Hsiao JK, Morrison PF, Bungay PM, Mefford IN, Scully MM, Dedrick RL (1992) Quantitative examination of tissue concentration profiles associated with microdialysis. J Neurochem 58:931–940.

Esler WP, Stimson ER, Jennings JM, Vinters HV, Ghilardi JR, Lee JP, Mantyh PW, Maggio JE (2000) Alzheimer's disease amyloid propagation by a template-dependent dock-lock mechanism. Biochemistry 39:6288–6295.

Fagan AM, Younkin LH, Morris JC, Fryer JD, Cole TG, Younkin SG, Holtzman DM (2000) Differences in the Abeta40/Abeta42 ratio associated with cerebrospinal fluid lipoproteins as a function of apolipoprotein E genotype. Ann Neurol 48:201–210.

Farris W, Mansourian S, Chang Y, Lindsley L, Eckman EA, Frosch MP, Eckman CB, Tanzi RE, Selkoe DJ, Guenette S (2003) Insulin-degrading enzyme regulates the levels of insulin, amyloid beta-protein, and the beta-amyloid precursor protein intracellular domain in vivo. Proc Natl Acad Sci USA 100:4162–4167.

Games D, Adams D, Alessandrini R, Barbour R, Berthelette P, Blackwell C, Carr T, Clemens J, Donaldson T, Gillespie F, Guido T, Hagopian S, Johnson-Wood K, Khan K, Lee M, Leibowitz P, Lieberburg I, Little S, Masliah E, McConlogue L, et al. (1995) Alzheimer-type neuropathology in transgenic mice overexpressing V717F beta-amyloid precursor protein. Nature 373:523–527.

Ghiso J, Matsubara E, Koudinov A, Choi-Miura NH, Tomita M, Wisniewski T, Frangione B (1993) The cerebrospinal-fluid soluble form of Alzheimer's amyloid beta is complexed to SP-40, 40 (apolipoprotein J), an inhibitor of the complement membrane-attack complex. Biochem J 293:27–30.

Golde TE, Eckman CB, Younkin SG (2000) Biochemical detection of Abeta isoforms: implications for pathogenesis, diagnosis, and treatment of Alzheimer's disease. Biochim Biophys Acta 1502:172–187.

Hartley DM, Walsh DM, Ye CP, Diehl T, Vasquez S, Vassilev PM, Teplow DB, Selkoe DJ (1999) Protofibrillar intermediates of amyloid β-protein induce acute electrophysiological changes and progressive neurotoxicity in cortical neurons. J Neurosci 19:8876–8884.

Holtzman DM (2001) Role of apoe/Abeta interactions in the pathogenesis of Alzheimer's disease and cerebral amyloid angiopathy. J Mol Neurosci 17:147–155.

Holtzman DM, Bales KR, Tenkova T, Fagan AM, Parsadanian M, Sartorius LJ, Mackey B, Olney J, McKeel D, Wozniak D, Paul SM (2000) Apolipoprotein E isoform-dependent amyloid deposition and neuritic degeneration in a mouse model of Alzheimer's disease. Proc Natl Acad Sci USA 97:2892–2897.

Iwata N, Tsubuki S, Takaki Y, Watanabe K, Sekiguchi M, Hosoki E, Kawashima-Morishima M, Lee HJ, Hama E, Sekine-Aizawa Y, Saido TC (2000) Identification of the major Abeta1–42-degrading catabolic pathway in brain parenchyma: suppression leads to biochemical and pathological deposition. Nat Med 6:143–150.

Jacobson I, Sandberg M, Hamberger A (1985) Mass transfer in brain dialysis devices—a new method for the estimation of extracellular amino acids concentration. J Neurosci Methods 15:263–268.

Johnson-Wood K, Lee M, Motter R, Hu K, Gordon G, Barbour R, Khan K, Gordon M, Tan H, Games D, Lieberburg I, Schenk D, Seubert P, McConlogue L (1997) Amyloid precursor protein processing and A beta42 deposition in a transgenic mouse model of Alzheimer disease. Proc Natl Acad Sci USA 94:1550–1555.

Kamenetz F, Tomita T, Hsieh H, Seabrook G, Borchelt D, Iwatsubo T, Sisodia S, Malinow R (2003) APP processing and synaptic function. Neuron 37:925–937.

Kayed R, Head E, Thompson JL, McIntire TM, Milton SC, Cotman CW, Glabe CG (2003) Common structure of soluble amyloid oligomers implies common mechanism of pathogenesis. Science 300:486–489.

Maggio JE, Stimson ER, Ghilardi JR, Allen CJ, Dahl CE, Whitcomb DC, Vigna SR, Vinters HV, Labenski ME, Mantyh PW (1992) Reversible in vitro growth of Alzheimer disease beta-amyloid plaques by deposition of labeled amyloid peptide. Proc Natl Acad Sci USA 89:5462–5466.

Matsubara E, Frangione B, Ghiso J (1995) Characterization of apolipoprotein J-Alzheimer's A beta interaction. J Biol Chem 270:7563–7567.

Menacherry S, Hubert W, Justice Jr JB (1992) In vivo calibration of microdialysis probes for exogenous compounds. Anal Chem 64:577–583.

Meyer-Luehmann M, Stalder M, Herzig MC, Kaeser SA, Kohler E, Pfeifer M, Boncristiano S, Mathews PM, Mercken M, Abramowski D, Staufenbiel M, Jucker M (2003) Extracellular amyloid formation and associated pathology in neural grafts. Nat Neurosci 6:370–377.

Morgan ME, Singhal D, Anderson BD (1996) Quantitative assessment of blood-brain barrier damage during microdialysis. J Pharmacol Exp Ther 277:1167–1176.

Morris JC, Price AL (2001) Pathologic correlates of nondemented aging, mild cognitive impairment, and early-stage Alzheimer's disease. J Mol Neurosci 17:101–118.

Price DL, Sisodia SS, Borchelt DR (1998) Genetic neurodegenerative diseases: the human illness and transgenic models. Science 282:1079–1083.

Pype S, Moechars D, Dillen L, Mercken M (2003) Characterization of amyloid beta peptides from brain extracts of transgenic mice overexpressing

the London mutant of human amyloid precursor protein. J Neurochem 84:602–609.
Selkoe DJ (2001) Alzheimer's disease: genes, proteins, and therapy. Physiol Rev 81:741–766.
Shibata M, Yamada S, Kumar SR, Calero M, Bading J, Frangione B, Holtzman DM, Miller CA, Strickland DK, Ghiso J, Zlokovic BV (2000) Clearance of Alzheimer's amyloid-ss(1–40) peptide from brain by LDL receptor-related protein-1 at the blood-brain barrier. J Clin Invest 106:1489–1499.
Simmons LK, May PC, Tomaselli KJ, Rydel RE, Fuson KS, Brigham EF, Wright S, Lieberburg I, Becker GW, Brems DN (1994) Secondary structure of amyloid beta peptide correlates with neurotoxic activity in vitro. Mol Pharmacol 45:373–379.
Sisodia SS (1999) Alzheimer's disease: perspectives for the new millennium. J Clin Invest 104:1169–1170.
Sisodia SS, Koo EH, Hoffman PN, Perry G, Price DL (1993) Identification and transport of full-length amyloid precursor proteins in rat peripheral nervous system. J Neurosci 13:3136–3142.
St. George-Hyslop PH (2000) Genetic factors in the genesis of Alzheimer's disease. Ann NY Acad Sci 924:1–7.
Tanzi RE, Kovacs DM, Kim TW, Moir RD, Guenette SY, Wasco W (1996) The gene defects responsible for familial Alzheimer's disease. Neurobiol Dis 3:159–168.
Teplow DB (1998) Structural and kinetic features of amyloid beta-protein fibrillogenesis. Amyloid 5:121–142.
Walsh DM, Hartley DM, Kusumoto Y, Fezoui Y, Condron MM, Lomakin A, Benedek GB, Selkoe DJ, Teplow DB (1999) Amyloid beta-protein fibrillogenesis. Structure and biological activity of protofibrillar intermediates. J Biol Chem 274:25945–25952.
Walsh DM, Klyubin I, Fadeeva JV, Cullen WK, Anwyl R, Wolfe MS, Rowan MJ, Selkoe DJ (2002) Naturally secreted oligomers of amyloid beta protein potently inhibit hippocampal long-term potentiation in vivo. Nature 416:535–539.
Weggen S, Eriksen JL, Das P, Sagi SA, Wang R, Pietrzik CU, Findlay KA, Smith TE, Murphy MP, Bulter T, Kang DE, Marquez-Sterling N, Golde TE, Koo EH (2001) A subset of NSAIDs lower amyloidogenic Abeta42 independently of cyclooxygenase activity. Nature 414:212–216.
Wiltfang J, Esselmann H, Bibl M, Smirnov A, Otto M, Paul S, Schmidt B, Klafki HW, Maler M, Dyrks T, Bienert M, Beyermann M, Ruther E, Kornhuber J (2002) Highly conserved and disease-specific patterns of carboxyterminally truncated Abeta peptides 1–37/38/39 in addition to 1–40/42 in Alzheimer's disease and in patients with chronic neuroinflammation. J Neurochem 81:481–496.
Wisniewski T, Ghiso J, Frangione B (1997) Biology of A beta amyloid in Alzheimer's disease. Neurobiol Dis 4:313–328.
Wu JT, Tung JS, Thorsett ED, Pleiss MA, Nissen JS, Neitz J, Latimer LH, John V, Freedman S, Britton TC, Audia JE, Reel JK, Mabry TE, Dressman BA, Cwi CL, Droste JJ, Henry SS, McDaniel SL, Scott WL, Stucky RD, Porter WJ (1998) Preparation of cycloalkyl, lactam, lactone and related compounds for inhibiting b-amyloid peptide release and/or its synthesis. PCT Int Appl WO 9828268 A 2:889.
Yang DS, Smith JD, Zhou Z, Gandy SE, Martins RN (1997) Characterization of the binding of amyloid-beta peptide to cell culture-derived native apolipoprotein E2, E3, and E4 isoforms and to isoforms from human plasma. J Neurochem 68:721–725.
Zhang ET, Richards HK, Kida S, Weller RO (1992) Directional and compartmentalised drainage of interstitial fluid and cerebrospinal fluid from the rat brain. Acta Neuropathol (Berl) 83:233–239.